Hypomorphic PCNA mutation underlies a human DNA repair disorder

Emma L. Baple,[1] Helen Chambers,[2] Harold E. Cross,[3] Heather Fawcett,[4] Yuka Nakazawa,[5,6] Barry A. Chioza,[1] Gaurav V. Harlalka,[1] Sahar Mansour,[7] Ajith Sreekantan-Nair,[1] Michael A. Patton,[1] Martina Muggenthaler,[1] Phillip Rich,[8] Karin Wagner,[9] Roselyn Coblentz,[9] Constance K. Stein,[10] James I. Last,[11] A. Malcolm R. Taylor,[11] Andrew P. Jackson,[12] Tomoo Ogi,[5,6] Alan R. Lehmann,[4] Catherine M. Green,[2,13] and Andrew H. Crosby[1]

[1]Medical Research, RILD Wellcome Wolfson Centre, University of Exeter Medical School, Exeter, Devon, United Kingdom. [2]Department of Zoology, University of Cambridge, Cambridge, United Kingdom. [3]Department of Ophthalmology, University of Arizona College of Medicine, Tucson, Arizona, USA. [4]Genome Damage and Stability Centre, University of Sussex, Falmer, Brighton, United Kingdom. [5]Nagasaki University Research Centre for Genomic Instability and Carcinogenesis (NRGIC), Nagasaki, Japan. [6]Department of Molecular Medicine, Atomic Bomb Disease Institute, Nagasaki University, Nagasaki, Japan. [7]SW Thames Regional Genetics Service, St. George's Healthcare NHS Trust, London, United Kingdom. [8]Department of Neuroradiology, St. George's Hospital, London, United Kingdom. [9]Windows of Hope Genetic Study, Walnut Creek, Ohio, USA. [10]SUNY Upstate Medical University, Syracuse, New York, USA. [11]School of Cancer Sciences, College of Medical and Dental Sciences, University of Birmingham, Birmingham, United Kingdom. [12]MRC Human Genetics Unit, Institute of Genetics and Molecular Medicine, University of Edinburgh, Edinburgh, United Kingdom. [13]Wellcome Trust Centre for Human Genetics, University of Oxford, Oxford, United Kingdom.

Numerous human disorders, including Cockayne syndrome, UV-sensitive syndrome, xeroderma pigmentosum, and trichothiodystrophy, result from the mutation of genes encoding molecules important for nucleotide excision repair. Here, we describe a syndrome in which the cardinal clinical features include short stature, hearing loss, premature aging, telangiectasia, neurodegeneration, and photosensitivity, resulting from a homozygous missense (p.Ser228Ile) sequence alteration of the proliferating cell nuclear antigen (PCNA). PCNA is a highly conserved sliding clamp protein essential for DNA replication and repair. Due to this fundamental role, mutations in PCNA that profoundly impair protein function would be incompatible with life. Interestingly, while the p.Ser228Ile alteration appeared to have no effect on protein levels or DNA replication, patient cells exhibited marked abnormalities in response to UV irradiation, displaying substantial reductions in both UV survival and RNA synthesis recovery. The p.Ser228Ile change also profoundly altered PCNA's interaction with Flap endonuclease 1 and DNA Ligase 1, DNA metabolism enzymes. Together, our findings detail a mutation of PCNA in humans associated with a neurodegenerative phenotype, displaying clinical and molecular features common to other DNA repair disorders, which we showed to be attributable to a hypomorphic amino acid alteration.

Introduction

Maintenance of genomic integrity is fundamentally important for normal cell division and basic cellular biological processes. The molecular characterization of human DNA damage sensitivity disorders, such as ataxia telangiectasia (AT), xeroderma pigmentosum (XP), and Cockayne syndrome (CS), has provided unique insight into the cellular mechanisms required for DNA damage tolerance and repair, and their importance for human health. The key features of such syndromes include predisposition to premature aging, malignancy, neurodegeneration, immunodeficiency, photosensitivity, and growth insufficiency (1–4). The process of nucleotide excision repair (NER) consists of 2 DNA repair pathways that are crucial for the removal of bulky lesions in DNA, including photoproducts resulting from exposure to UV light. Transcription-coupled NER (TC-NER) rapidly undertakes preferential repair of DNA lesions on actively transcribed DNA strands and is deficient in CS and UV-sensitive syndrome (5). Global genome NER (GG-NER) removes photoproducts more slowly from across the genome and is deficient in XP and trichothiodystrophy (6). After DNA damage is detected, both NER processes involve the excision of about 30 nucleotides encompassing the damaged DNA, followed by repair synthesis of new DNA to replace the damaged section. Repair synthesis is absolutely dependent on the DNA polymerase accessory protein proliferating cell nuclear antigen (PCNA) (7). This protein's major cellular role is to recruit and retain the replicative DNA polymerases at the sites of DNA synthesis during DNA replication. It forms a homotrimeric ring encircling and freely sliding along the DNA helix. PCNA interacts with a large number of accessory proteins and acts as a protein recruitment platform to coordinate the multiple enzymatic activities required for DNA replication and repair (8).

In the current study, 4 individuals aged 11–31 years affected by a novel syndrome were identified from a single extended pedigree consisting of 2 kindreds within the Ohio Amish community (Figure 1). The principal features included neurodegeneration, postnatal growth retardation, prelingual sensorineural hearing loss, premature aging, ocular and cutaneous telangiectasia, learning difficulties, photophobia, and photosensitivity with evidence of predisposition to sun-induced malignancy. Phenotypic similarities with XP, CS, and AT were noted (Table 1). All 4 affected individuals displayed short stature ranging from –3.8 to –5.2 standard deviation score (SDS), with an absence of pubertal growth spurt in the 2 eldest individuals. Neurodegeneration was a consistent feature,

Conflict of interest: The authors have declared that no conflict of interest exists.
Citation for this article: *J Clin Invest.* 2014;124(7):3137–3146. doi:10.1172/JCI74593.

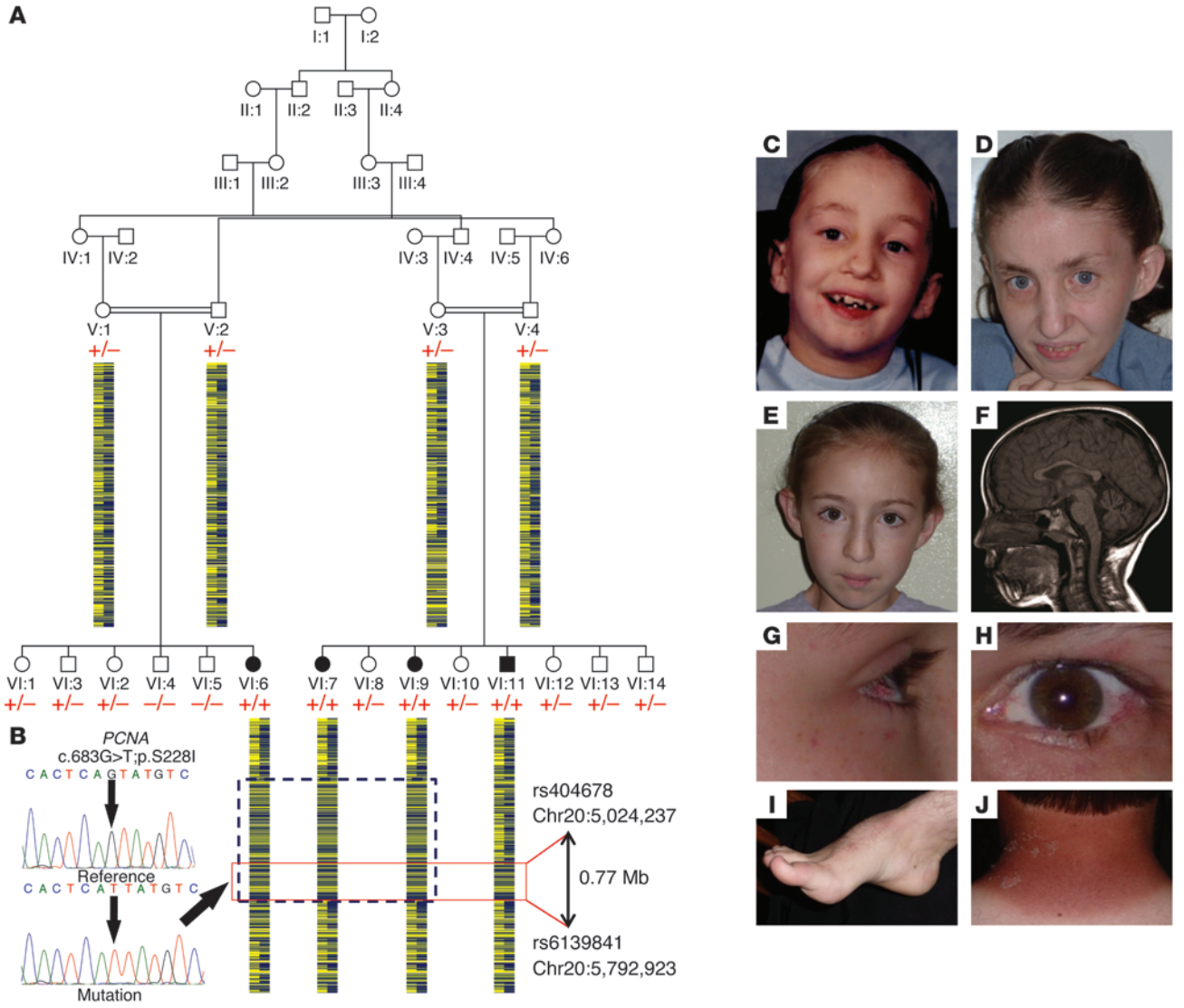

Figure 1

Family pedigree showing *PCNA* c.683G>T genotype data and images of affected individuals. (**A**) Simplified pedigree of the extended Amish family investigated, with pictorial representation of genotypes across ~6 Mb of chromosome 20 encompassing the disease locus (dashed blue boxed region, 2.72-Mb autozygous section in affected females; red boxed region, common 0.77-Mb region). Genotype is shown in red under individuals in generations V and VI (+, mutant; –, WT). All affected individuals were subsequently shown to be homozygous for the *PCNA* variant NM_002592.2 c.683G>T (indicated). Parental samples were heterozygous, and unaffected siblings were either WT or heterozygous carriers. (**B**) Electropherograms showing the DNA sequence at the position of *PCNA* c.683G>T in a WT control and a homozygous affected individual. (**C**–**J**) Clinical features of individuals homozygous for *PCNA* c.683G>T. (**C** and **D**) Patient VI:6 at 8 (**C**) and 31 (**D**) years of age, showing signs of premature aging. (**E**) Patient VI:7 at 11 years of age, with bilateral hearing aids in situ. (**F**) Midline sagittal T1-weighted brain scan of patient VI:9 at 8 years of age. Atrophy of the cerebellar vermis resulted in enlargement of vermian sulci and mild widening of the fourth ventricle. The brainstem was normal in appearance, and no supratentorial abnormality was noted. (**G** and **H**) Ocular and cutaneous telangiectasia in patients VI:7 and VI:11. (**I**) Pes cavus in patient VI:11. (**J**) Photosensitivity after minimal sun exposure in patient VI:11.

characterized by progressive gait instability, muscle weakness, foot deformity, difficulties with speech and swallowing, learning difficulties, and cognitive decline with advancing age. Prelingual onset of moderate to profound (worse at high frequency) sensorineural hearing loss was universal, a feature not commonly associated with the recognized DNA repair defects, and there was clear evidence of progression in patient VI:9. Muscle weakness was progressive; patient VI:6 had been wheelchair bound since the age of 16 years with contractures in all 4 limbs. Speech was unclear from onset and deteriorated with age; at the end of the present study, patient VI:6 had no speech and communicated with basic gestures. Progressive difficulty with swallowing solids/drooling was present in 3 of 4 affected patients. Neuroimaging was only available in 1 case (patient VI:7): MRI of the brain at 8 years of age demonstrated cerebellar atrophy involving the cerebellar vermis and hemispheres. Inner ear abnormalities included bilateral mild labyrinthine dysplasia with mildly dilated vestibules. All patients exhibited photophobia and photosensitivity, with evidence of premalignant changes in

Table 1
Clinical findings of individuals homozygous for *PCNA* c.683G>T and features of AT, CS, and the neurological form of XP

Trait	Patient VI:7	Disease VI:9	VI:11	VI:6	AT	CS	XP (neurological form)[A]
Gender, age (yr)	F, 11.5	F, 14.3	M, 26	F, 31			
Growth							
Short stature	–3.8 SDS	–5.2 SDS	–4.3 SDS	Substantial[B]	+	++	+
Head circumference (OFC)/ microcephaly	–3.2 SDS	–2.8 SDS	0.1 SDS	–2.8 SDS	–	++	+
Eyes							
Ocular telangiectasia	Present	Present	Present	Absent	++	–	–
Photophobia	Present	Present	Present	Present	–	+	++
Other eye abnormalities	Absent	Absent	Absent	UV-induced conjunctivitis	Oculomotor apraxia	Cataracts, pigmentary retinopathy, optic atrophy	UV-induced conjunctivitis, inflammatory lesions (limited to sun-exposed structures)
Skin							
Cutaneous telangiectasia	Present	Present	Present	Present	++	–	–
Photosensitivity	Present	Present	Present	Present	–/+	++	++
Predisposition to sunlight-induced skin cancer	Not known	Not known	Present	Not known	–/+	–	++
Neurology							
Developmental delay/ intellectual disability	Mild	Mild	Mild/ moderate	Severe	–/+	++	++
Ataxia/gait instability	Present	Present	Present	Present	++	++	+
Neurodegeneration	Present	Present	Present	Present	++	++	++
Cerebellar atrophy	Not known	Present	Not known	Not known	++	++[C]	++
Hearing loss	Present[D]	Present[D]	Present[D]	Present[D,E]	–	++[F]	++[F]
Additional features							
Premature aging	Not known	Not known	Absent	Present	+	++	++
Other physical findings	None	None	Absent pubertal growth spurt	Diaphragmatic hernia, absent pubertal growth spurt	Increased risk of leukemia and lymphoma	Incomplete puberty, dental caries	None

++, hallmark of the disease; +, sometimes associated with the disease; –, not associated with the disease. [A]About 25% of XP patients have neurological abnormalities (from groups A, D, F, and G). [B]Not possible to obtain accurate measurement. [C]Also hypomyelination and putaminal calcifications. [D]Prelingual. [E]Cognitive impairment prevented accurate assessment of severity. [F]Progressive, postlingual.

patient VI:11 (basal cell carcinoma in situ). All had several cutaneous telangiectasias, and 3 of 4 had conjunctival telangiectasia.

Assuming that a founder mutation was responsible for the condition, we used a combination of autozygosity mapping and linkage analysis to study this novel syndrome and identify the underlying molecular cause.

Results

A genome-wide SNP microarray scan of DNA from affected individuals and parents was undertaken. Inspection of resultant genotypes identified a single notable region of homozygosity of ~2.72 Mb on chromosome 20p13, shared solely by the 3 affected females. In the affected male, a de novo telomeric recombination event reduced this region to ~0.77 Mb, delimited by markers rs404678 and rs6139841 (NC_000020.10 g.5,024,237–5,792,923; Figure 1), likely to correspond to the disease locus (LOD_{max} 6.4). Microsatellite marker analysis confirmed autozygosity across this region (data not shown). We sequenced all 6 protein coding genes in the region (*PCNA*, *CDS2*, *PROKR2*, *GPCPD1*, *C20orf30*, and *C20orf196*), revealing a single potentially pathogenic sequence variant (NM_002592.2 c.683G>T) in exon 6 of *PCNA*. This variant, which cosegregated with the disease phenotype and was verified in the RNA transcript obtained from whole blood of an affected individual, was predicted to result in a substitution of a stringently conserved serine at position 228 for isoleucine (p.Ser228Ile) (Supplemental Figure 1; supplemental material available online with this article; doi:10.1172/JCI74593DS1). The variant was not detected in 360 control chromosomes of European ancestry, and only 2 heterozygous carriers were detected in the analysis of 310 Ohio Amish control chromosomes, which is not unexpected in this endogamous community. Only a single heterozygous carrier of European origin was identified in online sequencing project databases (1,000 Genomes Project and Exome Variant Server, ESP6500SI release). This single mutation carrier in 7,775 non-Amish individuals genotyped corresponds to a homozygous *PCNA* c.683T allele incidence in the region of approximately 1 in 241 million. We also subjected a single affected individual to whole exome sequence analysis (Otogenetics Corp.) to exclude other possible genetic causes. As expected, this confirmed the presence of the PCNA variant, but identi-

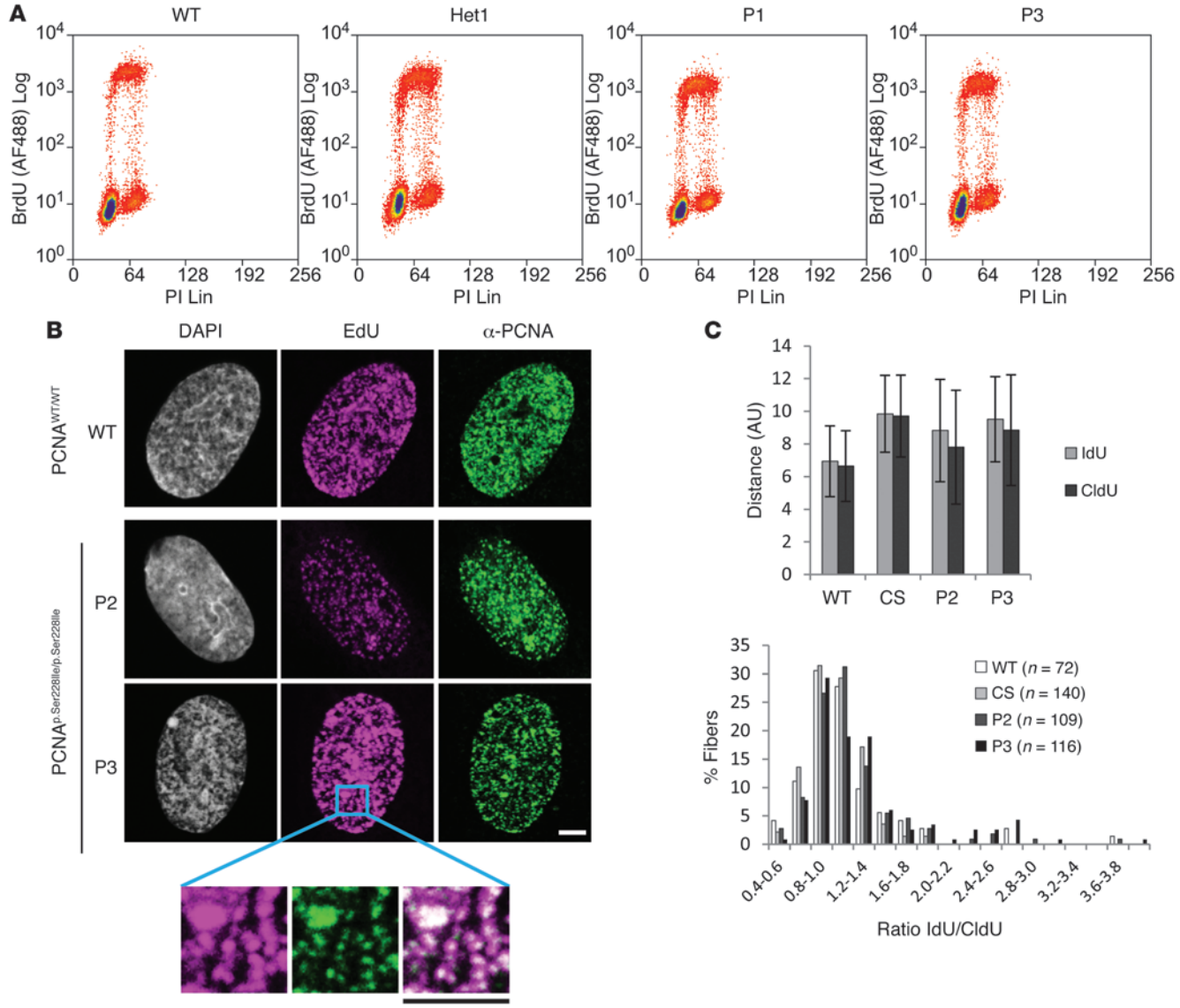

Figure 2

Cells homozygous for PCNA p.Ser228Ile have normal replication parameters. (**A**) FACS analysis of S phase in primary cells. Cells (passage <10) were labeled with BrdU for 30 minutes, and BrdU incorporation and DNA content were analyzed by FACS. No apparent differences were observed between cells from affected individuals (P1 and P3) and related (Het1) or unrelated (WT) control cells. Representative scatter plots are shown; each line was independently analyzed at least twice. (**B**) Immunofluorescence of primary control cells (WT) and affected individuals homozygous for PCNA p.Ser228Ile (P2 and P3). Right: Soluble proteins were removed by triton extraction prior to fixation, and cells were immunostained for PCNA. Middle: Sites of active DNA replication, visible as foci of incorporation of EdU. Enlargement shows colocalization between signals. Left: DNA was counterstained with DAPI. Scale bars: 3 μm. (**C**) Analysis of replication fork progression. Primary control cells, CS cells, and cells homozygous for PCNA p.Ser228Ile (P2 and P3) were incubated sequentially in medium supplemented with IdU and CldU, and the length of the DNA fiber replicated during each pulse was measured. Top: Comparable lengths of DNA were replicated during each pulse. Bottom: Similar frequency distribution of the IdU/CldU ratio within each fiber between cell lines. Error bars indicate SEM of 2 experiments.

fied no other known or possible pathogenic variants elsewhere, after excluding variants not compatible with recessive inheritance or cosegregating with the disease phenotype. Further conclusive support for the exclusion of diagnosis of AT and AT-like disorders was provided by our findings that included normal chromosomes (untreated or γ ray–induced; patient VI:11), alpha-fetoprotein (AFP) levels, Ig patterns (patients VI:7 and VI:9), and ataxia telangiectasia mutated (ATM) and associated protein and kinase activity levels (patients VI:6 and VI:11) in affected subjects (Supplemental Figures 2 and 3).

PCNA is an essential DNA replication accessory protein, highly conserved throughout evolution. It plays a central role at the replication fork, recruiting and retaining many of the enzymes required for DNA replication (8). Due to its fundamentally important cellular role, mutations that substantially affect PCNA protein function would be predicted to result in embryonic lethality. However, the survival of $PCNA^{Lys164Arg/Lys164Arg}$ knockin mice, generated to determine the role of PCNA lysine 164 modifications in somatic hypermutation, demonstrates that certain hypomorphic muta-

tions of PCNA can be tolerated in mammals (9). However, to our knowledge, no inherited human disorder arising from PCNA mutation has been previously described.

We therefore investigated the functional consequences of the PCNA p.Ser228Ile alteration. Primary fibroblasts (P-) were established from 3 affected individuals, patients VI:11, VI:9, and VI:7 (P1, P2, and P3, respectively), 2 heterozygous carriers (Het1 and Het2), and WT controls. EBV-transformed lymphoblastoid cells (L-) were established from 2 affected individuals, patients VI:11 and VI:6 (L5 and L6), 2 carriers (L8 and L10), and 2 Amish WT controls (L7 and L9). PCNA protein levels were unaltered in cells from affected individuals (Supplemental Figure 2). In order to assess the influence of the p.Ser228Ile alteration on DNA replication, we incubated primary fibroblasts (passage <10) with BrdU for 30 minutes and analyzed incorporation and DNA content by FACS (Figure 2A). No apparent differences were observed when comparing the fibroblasts from affected individuals with WT or heterozygote controls. During S phase, PCNA is recruited to so-called "DNA replication factories," the sites of nucleotide incorporation, which are visible as foci in the nuclei of replicating cells. Immunofluorescence analysis of endogenous PCNA in fibroblasts from affected individuals revealed no abnormalities in these foci (Figure 2B). In addition, no difference in replication fork rate was detected during unperturbed S phase using DNA fiber analysis (Figure 2C). Together, these data led us to conclude that the p.Ser228Ile variant does not dramatically interfere with the major replicative function of PCNA and that bulk DNA replication is not grossly perturbed.

Given that repair synthesis and downstream events of NER are absolutely dependent on PCNA (7), the reported photosensitivity in p.Ser228Ile homozygotes prompted us to examine the effect of the p.Ser228Ile substitution on cellular sensitivity to UV. Both primary fibroblasts and lymphoblastoid cells from affected individuals were more sensitive to UV irradiation than cells with WT PCNA (Figure 3, A and B), which suggests that the mutation specifically impairs the function of PCNA in DNA repair. To investigate this further, we evaluated GG-NER in primary fibroblast cell lines, measured by unscheduled DNA synthesis (UDS) assay (10). In cells from affected individuals, UDS was reproducibly reduced to approximately 50%–60% of normal values (Figure 3C). The level of RNA synthesis recovery (RRS) after UV radiation was used as a marker of TC-NER (11, 12). RRS was markedly decreased, to approximately 30%–50% of normal, in cells from affected individuals (Figure 3D and Supplemental Figure 4). The deficiency approached that of CS cells, which are known to be defective in TC-NER. Importantly, ectopic expression of WT PCNA fully rescued the RRS deficiency (Figure 3E), whereas it had only a minor effect on RRS in normal fibroblasts (Supplemental Figure 5), which demonstrated that the deficient UV responses were caused by the p.Ser228Ile sequence alteration. Although the 2 assays for UDS and RRS are by their nature different from each other and are semiquantitative, these results suggest that a subtle alteration in PCNA structure resulting from the p.Ser228Ile substitution is sufficient to specifically disrupt its role in NER, and this appears to have a more substantial effect on TC-NER.

Ser228 lies near the external face of PCNA (Figure 4A), and the mutation is therefore unlikely to affect its interaction with DNA. This residue is also distant from the regions of PCNA that mediate the formation of the trimeric ring structure (13). Consistent with this, no differences in trimer formation or stability between recombinant PCNA WT and p.Ser228Ile proteins were detected using gel filtration or glycerol gradient sedimentation (data not shown), and the amount of chromatin-associated PCNA (resistant to detergent extraction) was similar in WT and p.Ser228Ile homozygous cells. Interestingly, however, the altered residue is close to the interdomain connecting loop (IDCL) region, which mediates the interaction of PCNA with many of its protein partners. PCNA partner proteins, including DNA polymerase delta (PolD), DNA Ligase 1 (Lig1), and Flap endonuclease 1 (Fen1), often contain a PCNA-interacting protein (PIP) box, a sequence motif that mediates the IDCL interaction (14). In published crystal structures, Ser228 does not directly contact the PIP box–containing peptide (13, 15), although its close proximity to the interaction region may generate subtle positional alterations within this crucial domain, with functional consequences.

To determine whether specific protein interactions are perturbed by the p.Ser228Ile alteration, we performed a stable isotope labeling by aas in culture (SILAC) affinity purification assay. Extracts were made from HeLa cells grown in either normal medium or SILAC medium containing "heavy" amino acids ($[^{13}C_6/^{15}N_2]$ lysine and $[^{13}C_6/^{15}N_4]$ arginine). These extracts were individually exposed to affinity columns composed of recombinant PCNA (WT or p.Ser228Ile). Proteins that bound to each column were eluted, the eluates were combined, and the relative binding to each column was determined by mass spectrometry. This identified clear perturbations in the interaction of PCNA p.Ser228Ile with a limited number of interacting partners, most strikingly Fen1 and Lig1 (Figure 4B and Supplemental Table 1). This experiment revealed relatively increased amounts of Fen1 and Lig1 in the 500 mM eluates from the p.Ser228Ile compared with the WT column. To investigate this unexpected finding further, we analyzed the salt resistance of the PCNA-Fen1 interaction. HeLa nuclear extract was incubated with His-tagged PCNA (WT or p.Ser228Ile) beads, which were then washed with increasing NaCl up to 500 mM. The material eluted at 1 M NaCl and that retained on the beads was subsequently analyzed by Western blot for Fen1, which clearly demonstrated that the interaction between Fen1 and WT PCNA was much more resistant to high salt concentrations than the interaction between Fen1 and PCNA p.Ser228Ile (Figure 4C). This led us to conclude that in the SILAC experiments (Figure 4B), Fen1 remained bound to the WT PCNA column during the elution with 500 mM NaCl, resulting in a dramatic reduction of this protein in the WT eluate. Our conclusion that the p.Ser228Ile change impairs the ability of PCNA to bind Fen1 was further validated by subsequent immunoprecipitation and GST pulldown experiments (see below).

We assessed the effects of the PCNA p.Ser228Ile alteration in a more physiological setting by immunoprecipitation from lymphoblastoid cell extracts. While an interaction between Fen1 and PCNA was clearly demonstrated in controls, an intermediate level of interaction was detected in heterozygote cell lines, and the interaction was barely detectable in cells homozygous for PCNA p.Ser228Ile (Figure 4D). These data provided unambiguous confirmation that interaction of Fen1 with PCNA is dramatically reduced by the p.Ser228Ile mutation.

We have been unable to identify a commercially available antibody against Lig1 that is effective for immunoprecipitation from our lymphoblastoid extracts. Thus, in order to further investigate the effect of the PCNA p.Ser228Ile alteration on the interaction between PCNA and Lig1, we used an in vitro approach (16). Lysates

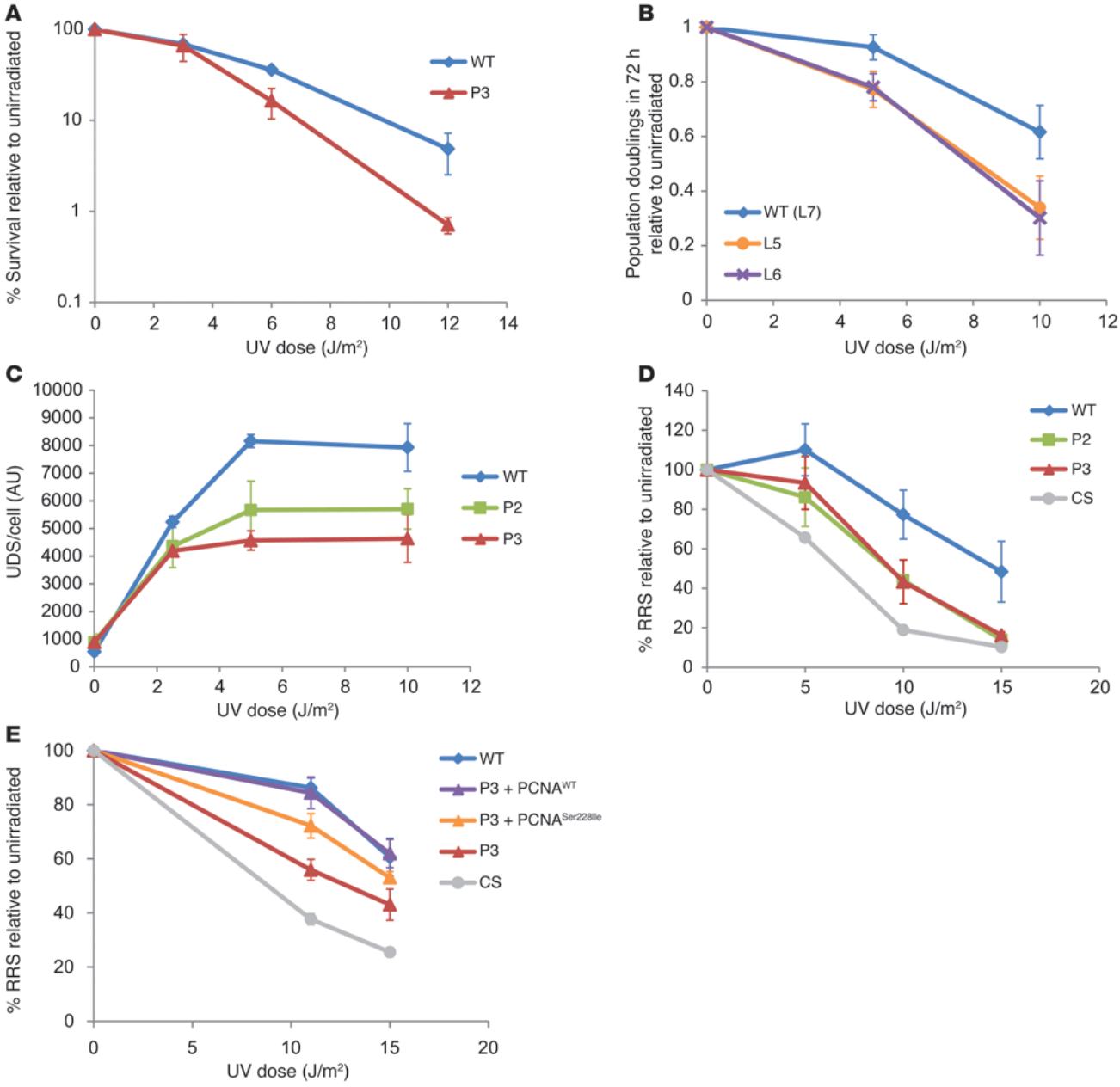

Figure 3

Abnormal cellular responses to UV. (**A**) Primary fibroblasts from an affected individual were sensitive to UV. Cell survival was measured by colony-forming ability after exposure to the indicated doses of UVC. (**B**) Lymphoblastoid cells from 2 different affected individuals were sensitive to UV. Viable cells were counted 72 hours after exposure to UVC using trypan blue exclusion. (**C**) Cells from affected individuals had reduced UDS activity. UDS was measured by incorporation of radiolabeled thymidine immediately after UV irradiation of nondividing cells with the indicated doses of UVC. (**D**) RRS, measured by incorporation of radiolabeled uridine 24 hours after UVC irradiation of nondividing cells with the indicated doses. A typical response of cells from a CS patient is shown for reference. (**E**) Defective RRS was complemented by lentiviral transduction of primary patient fibroblasts with WT PCNA. RRS was measured using EdU incorporation and automated high content microscopy in cells expressing high levels of ectopic PCNA. Values are mean and range of 2 experiments (**A**) or mean ± SEM of 3 (**B**–**D**) or 4 (**E**) experiments.

were prepared from *E. coli* expressing a fusion protein consisting of GST and the PIP box motif of either Fen1 or Lig1. These were then mixed with lysate containing PCNA (WT or p.Ser228Ile), glutathione beads were added, and the proteins associated with the beads were analyzed by SDS-PAGE. This assay recapitulated the defective interaction between PCNA p.Ser228Ile and Fen1 and, most significantly, showed that PCNA p.Ser228Ile also had a reduced affinity for the PIP box of Lig1 (Figure 4, E and F).

Given that Fen1 and Lig1 are both implicated in the NER pathways (17, 18), it is plausible that the cellular NER defects observed in cells from affected individuals result from the compromised interactions of these proteins with PCNA p.Ser288Ile. It also

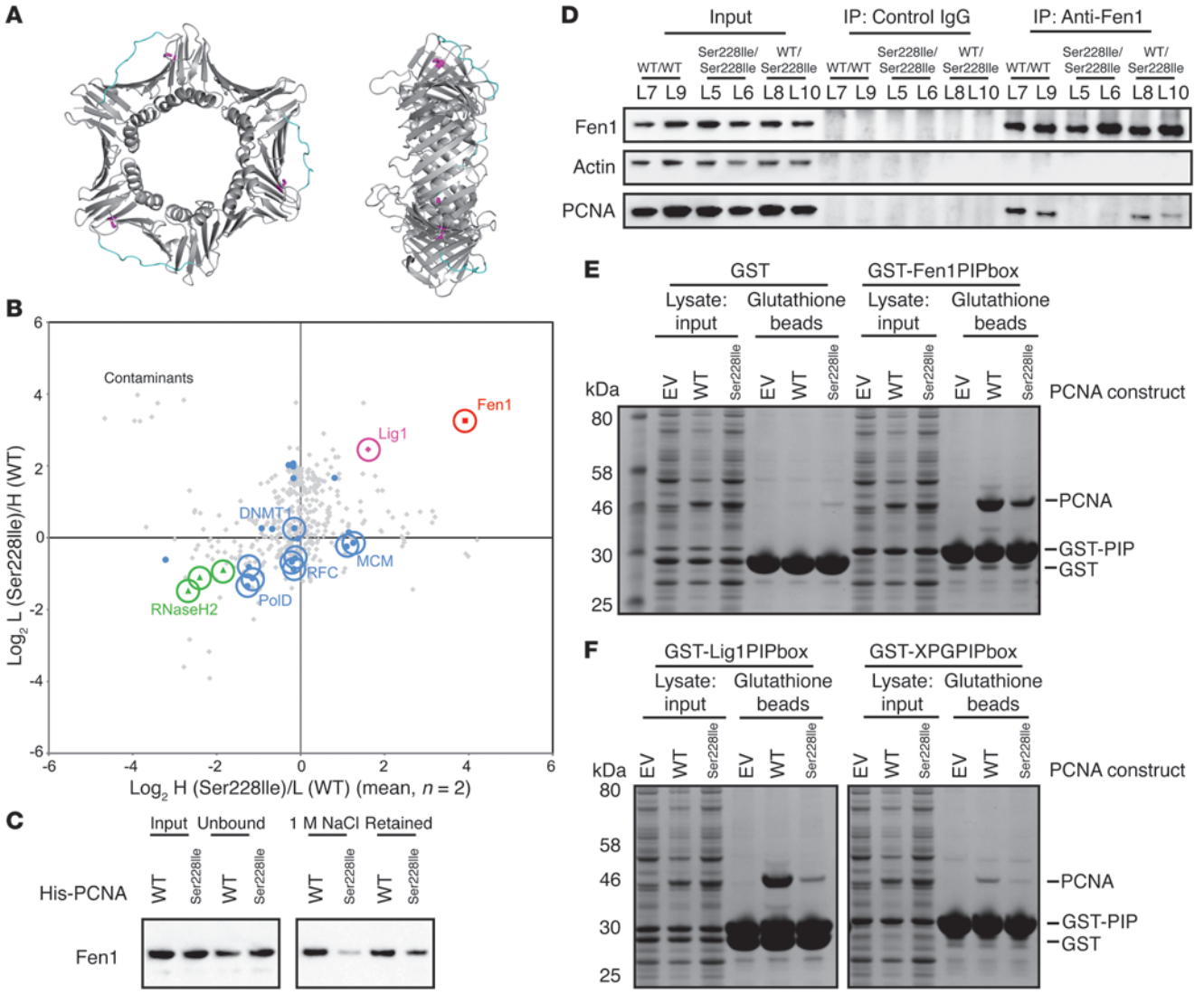

Figure 4

Perturbed PCNA interactions resulting from the p.Ser228Ile mutation. (**A**) Front and side views of the PCNA homotrimer, with Ser228 highlighted in magenta and the IDCL highlighted in cyan. Image was generated using POLYVIEW-3D (40), based on the 1YM crystal structure, rendered using PyMol. (**B**) Graphical representation of SILAC-based comparative PCNA-interaction analyses. Lysine [$^{13}C_6/^{15}N_2$] and arginine [$^{13}C_6/^{15}N_4$] labeled ("heavy"; H) or unlabeled ("light"; L) cell extracts were purified on PCNA WT or p.Ser228Ile affinity columns, and eluted proteins were analyzed by mass spectrometry. Each point represents the observed heavy/light ratios of a protein present in 3 of 3 experiments. Known PCNA-interacting proteins are shown in blue (see Supplemental Table 1). Proteins of particular interest are identified by name. (**C**) Recombinant His-PCNA (WT or p.Ser228Ile) was added to HeLa cell extracts and proteins bound to Ni-NTA. Proteins eluted at 1M NaCl or retained on the beads were analyzed by Western blot for Fen1. (**D**) Anti-Fen1 immunoprecipitates, from extracts made from lymphoblastoid lines derived from affected individuals or family members, were analyzed by Western blot for the presence of PCNA, Fen1, and actin. PCNA was almost undetectable in the precipitation from cell extracts derived from affected individuals. (**E**) *E. coli* lysates expressing empty vector (EV) or PCNA (WT or p.Ser228Ile) were mixed with lysates expressing GST or GST fused to the PIP box of Fen1. Inputs and glutathione-purified proteins were analyzed by SDS-PAGE and Coomassie staining. (**F**) Similar to **E**, except GST fusions comprising the PIP box of Lig1 and XPG were used.

seemed likely that the p.Ser228Ile alteration would perturb the PCNA interaction with other PIP box–containing partners and that this may contribute to the cellular phenotypes observed. One clear candidate, which is known to be required for NER and also to bind PCNA through a PIP box interaction, is XPG (16). We did not detect peptides derived from XPG in our SILAC assay, which by its nature will only detect relatively abundant proteins and relatively strong interactions. In the absence of an XPG antibody suitable for immunoprecipitation of endogenous XPG, the GST assay was again used to assess the binding of PCNA (WT and p.Ser228Ile) to the PIP box of XPG. Crucially, although less WT PCNA was bound to the XPG PIP box compared with its binding to the Fen1 PIP box, PCNA p.Ser228Ile displayed no detectable interaction with the XPG PIP box (Figure 4F). Thus, it seems reasonable to suggest that a defective interaction with XPG is also likely to contribute to the NER phenotype seen in cells homozygous for PCNA p.Ser228Ile.

Discussion

The genetic and cellular data described here implicated PCNA in a new, distinct neurodegenerative DNA repair disorder displaying some features in common with other conditions associated with deficient DNA metabolism, including CS, XP, and AT. The most notable similarities among CS, the neurological form of XP, and the individuals with the PCNA mutation described herein included growth abnormalities, premature aging, cognitive decline, photosensitivity, and photophobia. The presence of a basal cell carcinoma in situ in 1 affected individual (patient VI:11) likely indicates a predisposition to sun-induced malignancy in individuals homozygous for PCNA p.Ser228Ile and further clinical overlap with XP. However, the phenotype associated with PCNA p.Ser228Ile appears to be generally milder than that seen with typical CS or XP; most notably, the rate of premature aging seemed to be slower, with none of the ophthalmic manifestations associated with CS reported, and the effects of UV sensitivity appeared less substantial. Interestingly, although hearing loss is found in CS and some XP patients, the age of onset is typically later (1, 4). Thus, prelingual sensorineural hearing loss may, in association with the other clinical features described, be a helpful diagnostic feature in patients with this condition. The ocular and cutaneous telangiectasia seen in patients with the PCNA p.Ser228Ile mutation are reminiscent of those seen in AT, as was the pattern and progression of neurological abnormalities, although as with CS and XP, PCNA p.Ser228Ile homozygotes generally appeared to be less severely affected than typical AT patients. As with CS and XP, there were also striking differences between the phenotype associated with PCNA p.Ser228Ile and AT, including an absence of both the immunodeficiency and oculomotor apraxia commonly seen in AT-affected individuals.

Complete disruption of PCNA in flies or yeast is lethal (19, 20), an expected finding given its fundamental involvement in DNA replication. Until now, no pathological mutations in *PCNA* have been reported in human populations. In other species, however, some mutations of *PCNA* are compatible with life. For example, point mutations have been produced in *POL30* (encoding *S. cerevisiae* PCNA) that result in a wide variety of phenotypes, including DNA damage sensitivity, alterations in mutation rate, and epigenetic silencing defects (21). Similar phenotypes are seen in the various reported mutations in *mus209* (encoding *Drosophila* PCNA) (19). The only previously reported pathological mutation of *PCNA* in mammalian systems is a targeted missense mutation of lysine 164 to arginine (p.Lys164Arg) in mice, which was generated to assess the role of ubiquitination at this residue in somatic hypermutation in the immune system (9). Ubiquitination of PCNA at Lys164 is essential for translesion synthesis, a DNA damage tolerance process (22). Mice homozygous for *Pcna* p.Lys164Arg are viable but infertile and have an altered mutation spectrum of hypermutated Ig genes (9, 23). Thus, a subtle mutation of *PCNA* that impinges on a specific function can lead to characteristic loss-of-function effects on DNA metabolism.

Consistent with this, our present assays suggested that the PCNA p.Ser228Ile mutation described here is hypomorphic in nature. We did not detect any gross abnormalities of DNA replication associated with this mutation. Instead, we showed that the mutation had distinctive consequences for the cellular responses to UV, affecting both GG-NER and TC-NER. The effects on RRS seen in CS cell lines and on UDS in XP cell lines were typically more dramatic than we observed in homozygous PCNA p.Ser228Ile cells. This may explain, at least in part, why the phenotypic manifestations associated with these cellular abnormalities were not as profound in the individuals described herein compared with those seen in CS and XP.

Our findings defined particular defective interactions of PCNA p.Ser228Ile that are likely to be at least partly responsible for the specific alterations in cellular activities we observed, possibly together with other interactions not yet recognized. The altered protein interaction capability of PCNA p.Ser228Ile is also likely to account for the clinical manifestations of this syndrome. Complete abrogation of the PCNA-Fen1 interaction, mediated by a homozygous mutation of the Fen1 PIP box, is lethal in mice (24). Hence, it seems likely that while the p.Ser228Ile alteration dramatically reduces the association between PCNA and Fen1 in cell extracts, it is unlikely to completely abrogate their functional partnership. Consistent with this, our SILAC and interaction assays using recombinant proteins both showed that PCNA p.Ser228Ile remained capable of interacting with Fen1, although with markedly altered affinity. We cannot conclude from our assays whether the defective interactions with XPG, Fen1, and Lig1 are solely responsible for the observed effects on NER, although it is important to note that all these proteins are reported to be involved in this repair pathway (6, 17, 18). Thus, the perturbation of their interactions with PCNA could well be a major contributor to this abnormal cellular phenotype.

Mutations in XPG are rare and can be divided into 2 categories: missense mutations in the nuclease domains abrogate NER, but result in relatively mild XP phenotypes, whereas truncating mutations cause a very severe XP/CS complex disorder (25, 26). The *xpg*$^{-/-}$ mouse is barely viable (27). These varying phenotypes are thought to result because, in addition to its function in NER, XPG is involved in other processes (26). In particular, it associates with the transcription factor TFIIH and RNA polymerase II and has a role in transcription (25, 28, 29). The disruption of these other functions of XPG is suspected to be responsible for the more severe features of truncation mutations. For example, previously described patient XPCS1RO (94RD27) had severe early-onset CS and died at 7 months of age. He was homozygous for a frameshift mutation at codon 926 of *XPG*. This mutation leaves the nuclease domains intact, but truncates the protein before the PIP box and nuclear localization signal (30). Thus, the C-terminal region of XPG, including the motif responsible for interacting with PCNA, is very important for XPG function. These observations lead us to suggest that perturbation of PCNA's interaction with XPG may contribute to the neurological features associated with PCNA p.Ser228Ile.

In contrast to the homozygous state, mice heterozygous for the Fen1 PIP box mutant are viable, although they show predisposition to malignancy (31). Although specific PIP box mutations of Lig1 have not been generated in mammals, loss-of-function mutations in *LIG1* have been reported in a single individual, resulting in a complex human phenotype consisting of growth restriction, immunodeficiency, and photosensitivity (32), features reminiscent of those seen in PCNA p.Ser228Ile homozygotes. It is possible that Lig1 deficiency and PCNA p.Ser228Ile homozygosity together represent a group of conditions caused by disruption of multiple different DNA repair pathways. In addition, while the observed cellular defects correlated with the CS- and XP-like features of the syndrome, the clinical overlap with AT will require further investigation.

As well as being crucial to the maintenance of genomic integrity and prevention of neoplastic changes, DNA repair is known to be fundamentally important both during the rapid proliferative phase

characteristic of early neurogenesis and in the prevention of early cell death. The affected individuals with the PCNA mutation described herein displayed signs of neurodegeneration, a recognized feature of CS, AT, and neurological forms of XP, although the pathological patterns seen in each are distinct. More detailed investigation of the altered biological processes resulting from the PCNA p.Ser228Ile alteration should provide invaluable insight into the biological basis of this novel human disorder, as well as the neurodegenerative disease mechanisms involved in DNA damage tolerance and repair disorders. Further, although mutations resulting in complete loss of function of PCNA in humans may be incompatible with life, it remains an intriguing possibility that additional sequence variants in this gene, affecting other distinct aspects of PCNA function, might be viable and result in a phenotype more — or, indeed, less — severe than that associated with the p.Ser228Ile alteration described here.

Methods

Genetic studies. SNP genotyping was carried out using Illumina Human CytoSNP-12v2.1 330K arrays. Multipoint linkage analysis was performed with MERLIN (33) under a model of autosomal-recessive inheritance with full penetrance, assuming a disease allele frequency of 0.0001. Unique primers for sequencing and microsatellite analysis (Sigma-Aldrich) were designed using online software Primer3web (34) using sequences from the UCSC Genome Browser. RT-PCR was carried out using Clontech One Step RT-PCR Kit following the manufacturer's instructions, and bidirectional dideoxy DNA sequencing was performed on an ABI3130 XLA capillary sequencer (Applied Biosystems) with analysis using Finch TV 1.4.0 (Geospiza Inc.) and Gene Tool 1.0.0.1 (Bio Tools Inc.). Whole exome sequencing was performed by Otogenetics Corp. using the SureSelect Human All Exon V4 (Agilent Technologies) exome enrichment kit on an Illumina HiSeq2000. The exome sequencing produced 31,783,299 mapped reads, corresponding to 93% of targeted sequences covered sufficiently for variant calling (>10× coverage; mean depth, 45×).

Cell studies. Cells were cultured in DMEM/RPMI (Sigma Aldrich) with 15% FBS (FCS-Hyclone), 2 mM glutamine (Invitrogen), and 1% penicillin and streptomycin. UV sensitivity of lymphoblastoid cells was determined by irradiating cells in PBS (1×10^6 viable cells in 1 ml) with UVC (254 nm, 1 $Jm^{-2}s^{-1}$), adding 4 ml growth medium and counting viable cells using trypan blue exclusion after a 72-hour recovery period. UDS, RNA synthesis, fibroblast survival assays, and lentivirus-mediated complementation were performed as described previously (10–12, 35–37).

Protein interaction analyses. Recombinant PCNA WT and PCNA p.Ser228Ile were produced with a His-tag from pET28b in *E. coli* BL21 codonplus (Novagen) and purified on Ni-NTA sepharose (QIAGEN). Affinity columns were made by covalently linking these proteins to NHS-activated sepharose (Pierce). For SILAC analysis, HeLa cells were grown in SILAC DMEM (Gibco) supplemented with 10% dialyzed FBS, 2 mM $CaCl_2$, 1 mM $MgSO_4$, 52 mg/l L-leucine, and 100 mg/l L-lysine and L-arginine (for "heavy" extracts, we substituted [$^{13}C_6/^{15}N_2$] lysine and [$^{13}C_6/^{15}N_4$] arginine; CKgas). Extracts were made by lysing cells in a low-salt buffer containing benzonase (Merck), then adjusting to 150 mM NaCl. All protein interaction assays were performed in interaction buffer (25 mM Tris pH 7.5, 25 mm NaCl, 10% glycerol, 0.01% Igepal, 1 mM PMSF). Proteins eluted from PCNA affinity columns with 500 mM NaCl were combined before 10-fraction mass spectrometric (MS-MS) analysis (MS Bioworks). Data were analyzed, and H/L ratios were determined using MaxQuant software. To further analyze the stability of PCNA interactions, recombinant PCNAs were added to HeLa nuclear extract (4C), and complexes were isolated on Ni-NTA agarose and sequentially washed and eluted with increasing [NaCl]. For immunoprecipitation, protein extracts were made from lymphoblastoid cells as described above. Fen1 protein was precipitated using an anti-Fen1 rabbit antibody (EPR4459[2]; GeneTex) and protein A/G dynabeads (Invitrogen). Proteins in the extracts and precipitates were analyzed by Western blot with anti-PCNA (PC10; Abcam) or anti-Fen1 (4E7; GeneTex). GST fusion protein association studies were performed as previously described (16), using lysates from *E. coli* harboring pET30a as a control, or PCNA (WT or p.Ser228Ile) expressed from pET30a. These were mixed, in a buffer containing 100 mM KH_2PO_4/K_2HPO_4, with lysates from *E. coli* expressing glutathione S transferase (GST) or fusion proteins comprising GST and the PIP boxes of Fen1 (aa 328–355), XPG (aa 981–1,009), or Lig1 (aa 1–21 with an 8-aa glycine-serine spacer to maintain equal distance between the GST and the PIP box in all cases).

Western blotting. Exponentially growing primary human fibroblast cells were lysed on ice in 50 mM Tris-HCl pH 7.5, 150 mM NaCl, 200 μM EDTA, and 1% NP-40. Extracts were clarified by centrifugation at 10,000 *g* for 10 minutes at 4°C, then fractionated by SDS-PAGE. Proteins were transferred to Protran nitrocellulose (Whatman) and immunoblotted with anti-PCNA (PC10; Abcam) or anti-Fen1 (4E7; GeneTex). ATM kinase activity assay and Western blotting of ATM and associated proteins in lymphoblastoid cells was carried out as described previously (38).

FACS analysis of cell cycle position. Primary fibroblasts were incubated with 10 μM BrdU for 30 minutes, then trypsinized and fixed by addition of methanol to 70%. After storage at –20°C, cells were treated with 0.2 mg/ml pepsin in 2M HCl for 20 minutes, then incubated in 0.5% BSA in PBS with 0.5% Tween 20 and anti-BrdU antibody (1:50 dilution; BD) for 1 hour. Cells were then subjected to washing in 0.5% BSA and incubation with 1:100 anti-mouse secondary antibody coupled to Alexa Fluor 488 (Molecular Probes) for 30 minutes, followed by washing and resuspension in PBS with 0.5 mg/ml RNaseA for 15 minutes. Propidium iodide (10 μg/ml) was added just before analysis on a CyAn ADP Analyzer (Beckman Coulter Inc.).

Immunofluorescence. 5-ethynyl-2′-deoxyuridine (EdU) staining was carried out using the Click-iT EdU Alexa Fluor 555 Imaging Kit (Invitrogen). Cells were seeded onto glass coverslips so as to be subconfluent at the time of fixation. At least 24 hours after plating, EdU was added to the culture medium to a final concentration of 20 μM, and cells were returned to 37°C for 10 minutes. Soluble proteins were extracted by rinsing once in PBS and once in CSK buffer (100 mM NaCl, 300 mM sucrose, 10 mM PIPES pH 7.0, and 3 mM $MgCl_2$), then soaking in CSK plus 0.2% Triton X-100 for 5 minutes on ice. After a further wash in CSK, cells were fixed (ice-cold methanol for 20 minutes at –20°C), washed twice more in PBS, and then blocked (5% w/v BSA in PBST) for 30 minutes at room temperature. EdU staining was carried out according to the manufacturer's instructions. Coverslips were then incubated for 1 hour at room temperature in blocking buffer containing anti-PCNA monoclonal antibody (PC-10) diluted 1:1,000, followed by 3 washes in PBST and incubation in Alexa Fluor 488 goat anti-rabbit IgG (Invitrogen) diluted 1:1,000 in blocking buffer for 45 minutes. Cells were rinsed a further 3 times in PBST, and coverslips were mounted in Aqua-Poly/Mount (Polysciences) containing DAPI at a final concentration of 1.5 μg/ml. Slides were visualized using a Leica SP5 confocal microscope.

DNA fiber analysis. Immunolabeling of DNA fiber spreads was carried out as described previously (39), with minor modifications. Cells were incubated in 5-iodo-2′-deoxyuridine (IdU) and 5-chloro-2′-deoxyuridine (CldU) at a final concentration of 100 μM for 20 minutes each, and all antibody incubations were for 2 hours at room temperature. Fibers were mounted in ProLong mounting medium (Invitrogen).

Statistics. In graphical representations of experimental data, error bars represent SEM or range of the plotted mean of at least 2 independent experiments, as indicated in the figure legends.

Study approval. The present studies in humans were reviewed and approved (reference 10-0050-01) by the Institutional Review Board of the Office for the Responsible Conduct of Research, University of Arizona (Tucson, Arizona, USA). All tissue samples were taken with informed con-

sent in accordance with all ethical standards and protocols. Subjects or their guardians provided informed consent prior to their participation in the study. Written informed consent was obtained to publish the photographs of affected individuals.

Acknowledgments

We are grateful to the families for partaking in this study and to the Amish community for their continuing support of the Windows of Hope project. We are grateful to Luther Robinson for contributing clinical data, Kristiana Gordon for review of the dermatology, Wendy Albuquerque for review of the audiograms, and Jon Wing for technical assistance. Chromosome breakage studies were carried out at GSTS Pathology, and karyotyping was performed at South West Thames Genetics Laboratory. Illumina cytoSNP analysis and Sanger sequencing were carried out at the Medical Biomics Centre, St. George's University of London. FACS analysis was done by Drew Worth in the Flow Cytometry Core Facility of the Jenner Institute, Oxford. The work was supported by MRC Clinical Research Training fellowship G1001931 (to E.L. Baple), MRC grant G1002279 (to A.H. Crosby), MRC centenary fund award G0900205 (St. George's University of London, E.L. Baple), the Newlife Foundation for disabled children (to E.L. Baple and A.H. Crosby), Cancer Research UK career development fellowship C24125/A8307 (to C.M. Green), and Wellcome Trust Core Award 090532/Z/09/Z (to C.M. Green).

Received for publication December 4, 2013, and accepted in revised form April 17, 2014.

Address correspondence to: Andrew H. Crosby, Medical Research (Level 4), RILD Wellcome Wolfson Centre, Royal Devon and Exeter NHS Foundation Trust, Barrack Road, Exeter EX2 5DW, United Kingdom. Phone: 1392.408302; Fax: 1392.408388; E-mail: A.H.Crosby@exeter.ac.uk. Or to: Catherine M. Green, Wellcome Trust Centre for Human Genetics, University of Oxford, Roosevelt Drive, Oxford OX3 7BN, United Kingdom. Phone: 1865.287510; Fax: 1865.287501; E-mail: catherine.green@well.ox.ac.uk.

1. DiGiovanna JJ, Kraemer KH. Shining a light on xeroderma pigmentosum. *J Invest Dermatol*. 2012; 132(3 Pt 2):785–796.
2. Perlman S, Becker-Catania S, Gatti RA. Ataxia-telangiectasia: diagnosis and treatment. *Semin Pediatr Neurol*. 2003;10(3):173–182.
3. Kamileri I, Karakasilioti I, Garinis GA. Nucleotide excision repair: new tricks with old bricks. *Trends Genet*. 2012;28(11):566–573.
4. Nance MA, Berry SA. Cockayne syndrome: review of 140 cases. *Am J Med Genet*. 1992;42(1):68–84.
5. Cleaver JE. Photosensitivity syndrome brings to light a new transcription-coupled DNA repair cofactor. *Nat Genet*. 2012;44(5):477–478.
6. Cleaver JE, Lam ET, Revet I. Disorders of nucleotide excision repair: the genetic and molecular basis of heterogeneity. *Nat Rev Genet*. 2009;10(11):756–768.
7. Shivji KK, Kenny MK, Wood RD. Proliferating cell nuclear antigen is required for DNA excision repair. *Cell*. 1992;69(2):367–374.
8. Moldovan GL, Pfander B, Jentsch S. PCNA, the maestro of the replication fork. *Cell*. 2007; 129(4):665–679.
9. Langerak P, Nygren AO, Krijger PH, van den Berk PC, Jacobs H. A/T mutagenesis in hypermutated immunoglobulin genes strongly depends on PCNAK164 modification. *J Exp Med*. 2007; 204(8):1989–1998.
10. Lehmann AR, Stevens S. A rapid procedure for measurement of DNA repair in human fibroblasts and for complementation analysis of xeroderma pigmentosum cells. *Mutat Res*. 1980;69(1):177–190.
11. Mayne LV, Lehmann AR. Failure of RNA synthesis to recover after UV irradiation: an early defect in cells from individuals with Cockayne's syndrome and xeroderma pigmentosum. *Cancer Res*. 1982; 42(4):1473–1478.
12. Nakazawa Y, et al. Mutations in UVSSA cause UV-sensitive syndrome and impair RNA polymerase IIo processing in transcription-coupled nucleotide-excision repair. *Nat Genet*. 2012;44(5):586–592.
13. Gulbis JM, Kelman Z, Hurwitz J, O'Donnell M, Kuriyan J. Structure of the C-terminal region of p21(WAF1/CIP1) complexed with human PCNA. *Cell*. 1996;87(2):297–306.
14. Warbrick E. PCNA binding through a conserved motif. *Bioessays*. 1998;20(3):195–199.
15. Bruning JB, Shamoo Y. Structural and thermodynamic analysis of human PCNA with peptides derived from DNA polymerase-delta p66 subunit and flap endonuclease-1. *Structure*. 2004; 12(12):2209–2219.
16. Gary R, Ludwig DL, Cornelius HL, MacInnes MA, Park MS. The DNA repair endonuclease XPG binds to proliferating cell nuclear antigen (PCNA) and shares sequence elements with the PCNA-binding regions of FEN-1 and cyclin-dependent kinase inhibitor p21. *J Biol Chem*. 1997; 272(39):24522–24529.
17. Araujo SJ, et al. Nucleotide excision repair of DNA with recombinant human proteins: definition of the minimal set of factors, active forms of TFIIH, and modulation by CAK. *Genes Dev*. 2000; 14(3):349–359.
18. Wu Z, et al. High risk of benzo[alpha]pyrene-induced lung cancer in E160D FEN1 mutant mice. *Mutat Res*. 2012;731(1–2):85–91.
19. Henderson DS, Banga SS, Grigliatti TA, Boyd JB. Mutagen sensitivity and suppression of position-effect variegation result from mutations in mus209, the Drosophila gene encoding PCNA. *EMBO J*. 1994;13(6):1450–1459.
20. Waseem NH, Labib K, Nurse P, Lane DP. Isolation and analysis of the fission yeast gene encoding polymerase delta accessory protein PCNA. *EMBO J*. 1992;11(13):5111–5120.
21. Zhang Z, Shibahara K, Stillman B. PCNA connects DNA replication to epigenetic inheritance in yeast. *Nature*. 2000;408(6809):221–225.
22. Kannouche PL, Wing J, Lehmann AR. Interaction of human DNA polymerase eta with monoubiquitinated PCNA: a possible mechanism for the polymerase switch in response to DNA damage. *Mol Cell*. 2004;14(4):491–500.
23. Langerak P, Krijger PH, Heideman MR, van den Berk PC, Jacobs H. Somatic hypermutation of immunoglobulin genes: lessons from proliferating cell nuclear antigenK164R mutant mice. *Philos Trans R Soc Lond B Biol Sci*. 2009;364(1517):621–629.
24. Zheng L, Dai H, Qiu J, Huang Q, Shen B. Disruption of the FEN-1/PCNA interaction results in DNA replication defects, pulmonary hypoplasia, pancytopenia, and newborn lethality in mice. *Mol Cell Biol*. 2007;27(8):3176–3186.
25. Clarkson SG. The XPG story. *Biochimie*. 2003; 85(11):1113–1121.
26. Scharer OD. XPG: its products and biological roles. *Adv Exp Med Biol*. 2008;637:83–92.
27. Harada YN, et al. Postnatal growth failure, short life span, and early onset of cellular senescence and subsequent immortalization in mice lacking the xeroderma pigmentosum group G gene. *Mol Cell Biol*. 1999;19(3):2366–2372.
28. Sarker AH, et al. Recognition of RNA polymerase II and transcription bubbles by XPG, CSB, and TFIIH: insights for transcription-coupled repair and Cockayne Syndrome. *Mol Cell*. 2005;20(2):187–198.
29. Ito S, et al. XPG stabilizes TFIIH, allowing transactivation of nuclear receptors: implications for Cockayne syndrome in XP-G/CS patients. *Mol Cell*. 2007; 26(2):231–243.
30. Nouspikel T, Lalle P, Leadon SA, Cooper PK, Clarkson SG. A common mutational pattern in Cockayne syndrome patients from xeroderma pigmentosum group G: implications for a second XPG function. *Proc Natl Acad Sci U S A*. 1997;94(7):3116–3121.
31. Zheng L, et al. Fen1 mutations that specifically disrupt its interaction with PCNA cause aneuploidy-associated cancer. *Cell Res*. 2011;21(7):1052–1067.
32. Barnes DE, Tomkinson AE, Lehmann AR, Webster AD, Lindahl T. Mutations in the DNA ligase I gene of an individual with immunodeficiencies and cellular hypersensitivity to DNA-damaging agents. *Cell*. 1992;69(3):495–503.
33. Abecasis GR, Wigginton JE. Handling marker-marker linkage disequilibrium: pedigree analysis with clustered markers. *Am J Hum Genet*. 2005; 77(5):754–767.
34. Rozen S, Skaletsky H. Primer3 on the WWW for general users and for biologist programmers. *Methods Mol Biol*. 2000;132:365–386.
35. Lehmann AR, Thompson AF, Harcourt SA, Stefanini M, Norris PG. Cockayne's syndrome: correlation of clinical features with cellular sensitivity of RNA synthesis to UV irradiation. *J Med Genet*. 1993; 30(8):679–682.
36. Arlett CF, Harcourt SA, Cole J, Green MH, Anstey AV. A comparison of the response of unstimulated and stimulated T-lymphocytes and fibroblasts from normal, xeroderma pigmentosum and trichothiodystrophy donors to the lethal action of UV-C. *Mutat Res*. 1992;273(2):127–135.
37. Nakazawa Y, Yamashita S, Lehmann AR, Ogi T. A semi-automated non-radioactive system for measuring recovery of RNA synthesis and unscheduled DNA synthesis using ethynyluracil derivatives. *DNA Repair (Amst)*. 2010;9(5):506–516.
38. Reiman A, et al. Lymphoid tumours and breast cancer in ataxia telangiectasia; substantial protective effect of residual ATM kinase activity against childhood tumours. *Br J Cancer*. 2011;105(4):586–591.
39. Unsal-Kacmaz K, et al. The human Tim/Tipin complex coordinates an Intra-S checkpoint response to UV that slows replication fork displacement. *Mol Cell Biol*. 2007;27(8):3131–3142.
40. Porollo A, Meller J. Versatile annotation and publication quality visualization of protein complexes using POLYVIEW-3D. *BMC Bioinformatics*. 2007;8:316.